Modeling for Chemical Vapor Deposition

Jürgen Geiser

Humboldt-Universität zu Berlin,
Department of Mathematics,
Unter den Linden 6, D-10099 Berlin, Germany
geiser@mathematik.hu-berlin.de

Abstract. In this paper we present the modeling and simulation of a chemical vapor deposition for metallic bipolar plates.
In the models we discuss the application of different ideas to simulate the transport of chemical reactants in the gas chamber. Based on the multi-scaling problem of the underlying physical behavior, we discuss adapted models in different domains and scales. We combine analytically motivated solutions on simplified domains with numerical solutions based on more complex domains.
The near-and-far-field context is based on the large scale, that can be done with continuous models, as convection-diffusion-reaction equations, and small scales, that are based on chemical and molecular models as Boltzmann equations.
As an expert system of different models, we deal with different problems. Numerical methods are described in the context of time- and space-discretization methods.
For the simulations we apply analytical as well as numercial methods to obtain results to predict the growth of thin layers.
The results are discussed with physical experiments to give a valid model for the assumed growth.

Keywords: Chemical vapor deposition, multi-scale problem, operator-splitting methods, stiff differential equations.
AMS subject classifications. 35K20, 35K25, 70G65, 74S10.

1 Introduction

We motivate our study by simulating a growth of a thin film that can be done by CVD (chemical vapor deposition) processes, see [18] and [21]. In the last years, due to the research in producing high-temperature films by depositing low pressurs, the processes have increased and the understanding of the control mechanism of such processes are very important. We present such a hierachy of model for low-temperature and low-pressure plasma, that can be used to implant or deposite thin layers of important materials, see [16], [23]. Because of the multi-scale problem of the flow and reaction processes, we propose multi-scale problems, that are divided into near field and far field models. In the near field

model, the plasma will be discussed as a problem of reacting heavy particles with their underlying drift. This model takes into account the atomic behavior and allows large Knudsen numbers. In the far field model, the plasma can be treated as a continuous flow model. We assume nearly vacuum and a diffusion dominated process. In such viscous flow regimes, we deal with small Knudsen numbers and a pressure of nearly zero. We concentrate on the far field model and apply the operator-splitting methods with respect to the dimensional and time-splitting. The reaction part can be treated with fast Runge-Kutta solvers, whereas the convection-diffusion parts are solved with splitting semi-implicit finite volume methods. The numerical results discuss the applications in the production of so-called metallic bipolar plates. Here we discuss analytical and numerical models.

The paper is outlined as follows.

In Section 2 we present our mathematical model and a possible reduced model for further approximations.

In Section 3 we discuss the time- and space-discretization methods. Further, in Section 4 we apply the splitting methods for decoupling the multiphysics equations to reduce the amount of computational work. The numerical experiments are given in Section 5. In Section 6 we briefly summarize our results.

2 Mathematical Model

In the following, the models are discussed in two directions of far field and near field problems:

1. Reaction-diffusion equations, see [16] (far field problem);
2. Boltzmann-Lattice equations, see [23] (near field problem).

The modeling is considered by the Knudsen Number (Kn), which is the ratio of the mean free path λ over the typical domain size L. For small Knudsen Numbers $Kn \approx 0.01 - 1.0$, we deal with a Navier-Stokes equation or with the convection-diffusion equation, see [17] and [20], whereas for large Knudsen Numbers $Kn \geq 1.0$ we deal with a Boltzmann equation, see [21].

2.1 Model for Small Knudsen Numbers (Far Field Model)

When gas transport is physically more complex because of combined flows in three dimensions, the fundamental equations of fluid dynamics become the starting point of the analysis. For our models with small Knudsen numbers, we can assume a continuum flow, and the fluid equations can be treated with a Navier-Stokes or especially with a convection-diffusion equation.

Three basic equations describe the conservation of mass, momentum, and energy, that are sufficient to describe the gas transport in the reactors, see [21].

1. Continuity: The conservation of mass requires that the net rate of the mass accumulation in a region has to be equal to the difference between the inflow and outflow rate.

2. Navier-Stokes: The momentum conservation requires that the net rate of momentum accumulation in a region has to be equal to the difference between the in and out rate of the momentum, plus the sum of the forces acting on the system.
3. Energy: The rate of accumulation of internal and kinetic energy in a region is equal to the net rate of internal and kinetic energy by convection, plus the net rate of heat flow by conduction, minus the rate of work done by the fluid.

We will concentrate on the conservation of mass and assume that the energy and momentum is conserved, see [16]. Therefore the continuum flow can be described as a convection-diffusion equation given as:

$$\frac{\partial}{\partial t}c + \nabla F - R_g = 0, \text{ in } \Omega \times [0,T] \tag{1}$$

$$F = -D\nabla c,$$

$$c(x,t) = c_0(x), \text{ on } \Omega, \tag{2}$$

$$c(x,t) = c_1(x,t), \text{ on } \partial\Omega \times [0,T], \tag{3}$$

where c is the molar concentration and F the flux of the species. D is the diffusivity matrix and R_g is the reaction term. The initial value is given as c_0 and we assume a Dirichlet boundary with the function $c_1(x,t)$ being sufficiently smooth.

2.2 Model for Large Knudsen Numbers (Near Field Model)

The model assumes that the heavy particles can be described with a dynamical fluid model, where the elastic collisions define the dynamics and few inelastic collisions are, among other reasons, responsible for the chemical reactions.

To describe the individual mass densities as well as the global momentum and the global energy as dynamic conservation quantities of the system, corresponding conservation equations are derived from Boltzmann equations.

The individual character of each species is considered by mass-conservation equations and the so-called difference equations.

The Boltzmann equation for heavy particles (ions and neutral elements) is now given as

$$\frac{\partial}{\partial t}n_s + \frac{\partial}{\partial \boldsymbol{r}} \cdot (n_s \boldsymbol{u} + n_s c_s) = Q_n^{(s)}, \tag{4}$$

$$\frac{\partial}{\partial t}\rho \boldsymbol{u} + \frac{\partial}{\partial \boldsymbol{r}} \cdot \left(\rho \boldsymbol{u}\boldsymbol{u} + nT\underline{\underline{I}} - \underline{\underline{\tau}}^*\right) = \sum_{s=1}^{N} q_s n_s \langle \boldsymbol{E} \rangle,$$

$$\frac{\partial}{\partial t}\mathcal{E}_{\text{tot}}^* + \frac{\partial}{\partial \boldsymbol{r}} \cdot \left(\mathcal{E}_{\text{tot}}^* \boldsymbol{u} + \boldsymbol{q}^* + nT\boldsymbol{u} - \underline{\underline{\tau}}^* \cdot \boldsymbol{u}\right) = \sum_{s=1}^{N} q_s n_s \left(\boldsymbol{u} + \boldsymbol{c}_s\right) \cdot \langle \boldsymbol{E} \rangle - Q_{\mathcal{E},\text{inel}}^{(e)},$$

where ρ denotes the mass density, $\boldsymbol{u}$ is the velocity, and T the temperatur of the ions. $\mathcal{E}_{\text{tot}}^*$ is the total energy of the heavy particles. n_s is the particle density of

heavy particle species s. $\boldsymbol{q}^*$ is the heat flux of the heavy particle system. $\underline{\underline{\tau}}^*$ is the viscous stress of the heavy particle system. $\boldsymbol{E}$ is the electric field, and $Q_{\mathcal{E}}$ is the energy conservation.

Further the production terms are $Q_n^{(s)} = \sum_r a_{\text{sign}} k_{\alpha,r} n_\alpha n_r$ with the rate coefficients $k_{\alpha,r}$.

We have drift diffusion for heavy particles in the following fluxes. The dissipative fluxes of the impuls and energy balance are linear combinations of generalized forces,

$$\begin{aligned}
\boldsymbol{q}^* &= \lambda_E \langle \boldsymbol{E} \rangle - \lambda \frac{\partial}{\partial \boldsymbol{r}} T - \sum_{s=1}^{N} \sum_{\alpha=1}^{N} \lambda_n^{(\alpha,s)} \frac{1}{n_s} \frac{\partial}{\partial \boldsymbol{r}} n_\alpha, \\
\underline{\underline{\tau}}^* &= -\eta \left(\frac{\partial}{\partial \boldsymbol{r}} \boldsymbol{u} + \left(\frac{\partial}{\partial \boldsymbol{r}} \boldsymbol{u} \right)^\top - \frac{2}{3} \left(\frac{\partial}{\partial \boldsymbol{r}} \cdot \boldsymbol{u} \right) \underline{\underline{I}} \right), \\
\mathcal{E}_{\text{tot}}^* &= \sum_{s=1}^{N} 1/2 \rho_s c_s^2 + 1/2 \rho u^2 + 3/2 n T,
\end{aligned}$$

where λ is the thermal diffusion transport coefficient. T is the temperature, n is the particle density.

Diffusion of the species are underlying to the given plasma and described by the following equations

$$\begin{aligned}
\tfrac{\partial}{\partial t} n_s + \tfrac{\partial}{\partial \boldsymbol{r}} \cdot (n_s \boldsymbol{u} + n_s \boldsymbol{c}_s) &= Q_n^{(s)}, \\
\boldsymbol{c}_s = \mu_s \langle \boldsymbol{E} \rangle - d_T^{(s)} \tfrac{\partial}{\partial \boldsymbol{r}} T - \textstyle\sum_{\alpha=1}^{N} D_n^{(\alpha,s)} \tfrac{1}{n_s} \tfrac{\partial}{\partial \boldsymbol{r}} n_\alpha.
\end{aligned}$$

The density of the species are dynamical values and the species transport and mass transport are underlying to the following constraint conditions:

$$\begin{aligned}
\textstyle\sum_s m_s n_s &= \rho, \\
\textstyle\sum_s n_s m_s \boldsymbol{c}_s &= 0,
\end{aligned}$$

where m_s is the mass of the heavy particle, n_s is the density of the heavy particle, c_s is the difference velocity of the heavy particle.

Field Model

The plasma transport equations are maxwell equations and are coupled with a field. They are given as

$$\frac{1}{\mu_0} \nabla \times \boldsymbol{B}_{\text{dyn}} = -e n_e \boldsymbol{u}_e + \tilde{\boldsymbol{j}}_{\text{ext}}, \tag{5}$$

$$\nabla \cdot \boldsymbol{B}_{\text{dyn}} = 0, \tag{6}$$

$$\nabla \times \boldsymbol{E} = -\frac{\partial}{\partial t} \boldsymbol{B}_{\text{dyn}}, \tag{7}$$

where $\boldsymbol{B}$ is the magnetic field and $\boldsymbol{E}$ is the electric field.

2.3 Simplified Model for Large Knudsen Numbers (Near Field Model)

For the numerical analysis and for the computational results, we reduce the complex model and derive a system of coupled Boltzmann and diffusion equations.

We need the following assumptions:

$$\begin{aligned} \boldsymbol{q}^* &= -\lambda \frac{\partial}{\partial \boldsymbol{r}} T, \\ \underline{\underline{\tau}}^* &= 0, \\ \mathcal{E}^*_{\text{tot}} &= 3/2nT, \\ Q^{(e)}_{\mathcal{E},\text{inel}} &= \text{const}, \end{aligned}$$

and obtain a system of equations:

$$\frac{\partial}{\partial t}\rho + \frac{\partial}{\partial \boldsymbol{r}} \cdot (\rho \boldsymbol{u}) = 0,$$

$$\frac{\partial}{\partial t}\rho \boldsymbol{u} + \frac{\partial}{\partial \boldsymbol{r}} \cdot \left(\rho \boldsymbol{u}\boldsymbol{u} + nT\underline{\underline{I}}\right) = \sum_{s=1}^{N} q_s n_s \langle \boldsymbol{E} \rangle,$$

$$\frac{\partial}{\partial t} 3/2nT + \frac{\partial}{\partial \boldsymbol{r}} \cdot \left(3/2nT\boldsymbol{u} + \lambda \frac{\partial}{\partial \boldsymbol{r}} T + nT\boldsymbol{u}\right) = \sum_{s=1}^{N} q_s n_s \left(\boldsymbol{u} + \boldsymbol{c}_s\right) \cdot \langle \boldsymbol{E} \rangle - Q^{(e)}_{\mathcal{E},\text{inel}} \,.$$

Remark 1. We obtain three coupled equations for the density, velocity and the temperature of the plasma. The equations are strong coupled and a decomposition can be done in the discretized form.

In the following we describe the time- and space-discretization methods.

3 Discretization Methods

In the following we discuss the discretization methods, that are used for the far field model. We discuss the dicretization of the reaction term as an ODE with small scales and the convection-diffusion part as a PDE with large scales.

3.1 Discretization Methods for the Reaction Part

For the reaction part of the transport equation we need an accurate method, see [9] and [10].

Often the accuracy for the time-discretization of the split equation is necessary to combine two results of the equation. Thus we will fit in the higher-order methods.

Based on the iterative splitting methods the start solution for the first iteration step is important to obtain higher-order results. For the next iteration steps the order has to increase until the proposed order of the time-discretization is achieved.

Therefore we propose the Runge-Kutta and BDF methods as adapted time-discretization methods to reach higher-order results.

For the time-discretization we use the following higher-order methods.

Runge-Kutta Method We use the implicit trapezoidal rule:

$$\begin{array}{c|cc} 0 & & \\ 1 & \frac{1}{2} & \frac{1}{2} \\ \hline & \frac{1}{2} & \frac{1}{2} \end{array} \quad . \tag{8}$$

Furthermore we use the Gausequential splitting-Runge-Kutta method:

$$\begin{array}{c|cc} \frac{1}{2}-\frac{\sqrt{3}}{6} & \frac{1}{4} & \frac{1}{4}-\frac{\sqrt{3}}{6} \\ \frac{1}{2}+\frac{\sqrt{3}}{6} & \frac{1}{4}+\frac{\sqrt{3}}{6} & \frac{1}{4} \\ \hline & \frac{1}{2} & \frac{1}{2} \end{array} \quad . \tag{9}$$

To use these Runge-Kutta methods with our operator-splitting method we have to take into account, that we solve in each iteration step equations of the form $\partial_t u_i = Au_i + b$, where $b = Bu_{i-1}$ is a discrete function, as we only have a discrete solution for u_{i-1}.

For the implicit trapezoidal rule this is no problem, because we do not need the values at any subpoint. However, for the Gausequential splitting method we need to now the values of b at the subpoints $t_0 + c_1 h$ and $t_0 + c_2 h$ with $c = (\frac{1}{2} - \frac{\sqrt{3}}{6}, \frac{1}{2} + \frac{\sqrt{3}}{6})^T$. Therefore we must interpolate b. On that account we choose the cubic spline functions.

Numerical experiments show that this works properly with non-stiff problems, but not very well with stiff problems.

3.2 BDF method

Because the higher-order Gausequential splitting-Runge-Kutta method combined with cubic spline interpolation does not work properly for stiff problems, we use the BDF method of third order, which does not need any subpoints. Therefore no interpolation is needed.

The BDF3 method is defined by

$$\frac{1}{k}\left(\frac{11}{6}u^{n+2} - 3u^{n+1} + \frac{3}{2}u^n - \frac{1}{3}u^{n-1}\right) = A(u^{n+3}). \tag{10}$$

For the pre-stepping, i.e. to obtain u_1, u_2, we use the implicit trapezoidal rule (8).

Implicit-Explicit Methods The implicit-explicit (IMEX) schemes have been widely used for time integration of spatial discretized partial differential equations of diffusion-convection type. These methods are applied to decouple the implicit and explicit terms. Treating the convection-diffusion equation for example, one can use the explicit part for the convection and the implicit part for the diffusion term. In our application we divide between the stiff and non-stiff term. We apply the implicit part for stiff operators and the explicit part for non-stiff operators.

FSRK Method We propose the A-stable fractional-stepping Runge-Kutta (FSRK) scheme, see [1], of first and second order for our applications.
The tableau in the Butcher form is given as

$$\begin{array}{c|cccc|cccc} 1 & 1 & & & & 0 & & & \\ 1 & 1 & 0 & & & 0 & 1 & & \\ \frac{4}{9} & -\frac{88}{45} & 0 & \frac{12}{5} & 0 & 0 & \frac{5}{9} & 0 & \\ \frac{1}{3} & -\frac{407}{75} & 0 & -\frac{144}{25} & 0 & 0 & -\frac{31}{15} & 0 & \frac{12}{5} \\ \hline \text{order1} & 1 & 0 & 0 & 0 & 0 & 1 & 0 & 0 \\ \hline \text{order2} & \frac{1}{10} & 0 & \frac{9}{10} & 0 & 0 & \frac{1}{4} & 0 & \frac{3}{4} \end{array} . \tag{11}$$

To obtain second-order convergence in numerical examples it is important to split the operator in the right way as we will show later.

SBDF Method We use the following stiff backward differential formula (SBDF) method, which is a modification of the third-order backward differential formula (BDF3). As pre-stepping method we use again the implicit trapezoidal rule.

$$\begin{aligned} &\frac{1}{k}\left(\frac{11}{6}u^{n+1} - 3u^n + \frac{3}{2}u^{n-1} - \frac{1}{3}u^{n-2}\right) \\ &= 3A(u^n) - 3A(u^{n-1}) + A(u^{n-2}) + B(u^{n+1}). \end{aligned} \tag{12}$$

Again it is important to split the operator in the right way.

3.3 Discretization Methods for the Diffusion Equation

We discretize the diffusion-dispersion equation using the implicit time-discretization and finite volume method for the equation

$$\partial_t R\, c - \nabla \cdot (D \nabla c) = 0, \tag{13}$$

where $c = c(x,t)$ with $x \in \Omega$ and $t \geq 0$. The diffusions-dispersions tensor $D = D(x, \mathbf{v})$ is given by the Scheidegger approach, see [22]. The velocity is given as $\mathbf{v}$. The retardation factor is $R > 0.0$.

The boundary values are denoted by $\mathbf{n} \cdot D\, \nabla c(x,t) = 0$, where $x \in \Gamma$ is the boundary $\Gamma = \partial\Omega$, see [8]. The initial conditions are given by $c(x,0) = c_0(x)$.

We integrate the equation (13) over space and time and derive

$$\int_{\Omega_j} \int_{t^n}^{t^{n+1}} \partial_t R(c)\, dt\, dx = \int_{\Omega_j} \int_{t^n}^{t^{n+1}} \nabla \cdot (D \nabla c)\, dt\, dx.$$

The time-integration is done by the backward Euler method and the diffusion-dispersion term is lumped, cf. [12].

$$\int_{\Omega_j} (R(c^{n+1}) - R(c^n))\, dx = \tau^n \int_{\Omega_j} \nabla \cdot (D \nabla c^{n+1})\, dx. \tag{14}$$

The equation (14) is discretized over the space using Green's formula.

$$\int_{\Omega_j} (R(c^{n+1}) - R(c^n))\, dx = \tau^n \int_{\Gamma_j} D\, \mathbf{n} \cdot \nabla c^{n+1}\, d\gamma, \tag{15}$$

where Γ_j is the boundary of the finite volume cell Ω_j. We use the approximation in space, confer [12].

The space-integration for (15) is done by the mid-point rule over the finite boundaries and given as

$$V_j R(c_j^{n+1}) - V_j R(c_j^n) = \tau^n \sum_{e \in \Lambda_j} \sum_{k \in \Lambda_j^e} |\Gamma_{jk}^e| \mathbf{n}_{jk}^e \cdot D_{jk}^e \nabla c_{jk}^{e,n+1},$$

where $|\Gamma_{jk}^e|$ is the length of the boundary element Γ_{jk}^e. The gradients are calculated with the piecewise finite element function ϕ_l, and we obtain

$$\nabla c_{jk}^{e,n+1} = \sum_{l \in \Lambda^e} c_l^{n+1} \nabla \phi_l(\mathbf{x}_{jk}^e).$$

We get with the difference notation for the neighbor point j and l, cf. [7] the discretized equation

$$\begin{aligned} &V_j R(c_j^{n+1}) - V_j R(c_j^n) = \\ &= \tau^n \sum_{e \in \Lambda_j} \sum_{l \in \Lambda^e \setminus \{j\}} \Big(\sum_{k \in \Lambda_j^e} |\Gamma_{jk}^e| \mathbf{n}_{jk}^e \cdot D_{jk}^e \nabla \phi_l(\mathbf{x}_{jk}^e) \Big) (c_j^{n+1} - c_l^{n+1}), \end{aligned}$$

where $j = 1, \ldots, m$.

4 Splitting Methods

In the following we discuss the possible splitting methods for our problem. The multiscale problems of the reaction and diffusion operators are decoupled by the time splitting. The different scales of the diffusion operator are decoupled by a dimensional splitting method. In the following we discuss the decomposition methods for time and space as methods to obtain efficient and accurate solvers.

4.1 Time Splitting methods

In the following, splitting methods of first order are described. We consider linear ordinary differential equations

$$\partial_t c(t) = A\, c(t) \; + \; B\, c(t), \tag{16}$$

where the initial conditions are given as $c^n = c(t^n)$. The operators A and B are assumed to be bounded linear operators in the Banach space X with $A, B : X \to X$. In our case the operator A is the diffusion part, while B is the reaction part.

In the applications the operators correspond to the physical operators, e.g. the convection and diffusion operator.

The operator-splitting method is introduced as a method, which solves two equation parts sequentially, with respect to initial conditions. The method is given as following

$$\begin{aligned} \frac{\partial c^*(t)}{\partial t} &= Ac^*(t), \quad \text{with } c^*(t^n) = c^n, \\ \frac{\partial c^{**}(t)}{\partial t} &= Bc^{**}(t)\ , \quad \text{with } c^{**}(t^n) = c^*(t^{n+1}), \end{aligned} \tag{17}$$

where the time step is given as $\tau^n = t^{n+1} - t^n$. The solution of the equation (16) is $c^{n+1} = c^{**}(t^{n+1})$.

The splitting error of the method is derived with Taylor expansion, cf. [12]. We obtain the global error as

$$\begin{aligned} \rho_n &= \frac{1}{\tau}(\exp(\tau^n(A+B)) - \exp(\tau^n B)\exp(\tau^n A))\ c(t^n) \\ &= \frac{1}{2}\tau^n[A,B]\ c(t^n) + O((\tau^n)^2). \end{aligned} \tag{18}$$

where $[A,B] := AB - BA$ is the commutator of A and B. We get an error $\mathcal{O}(\tau^n)$ if the operators A and B do not commute, otherwise the method is exact.

To obtain higher-order splitting methods, we can deal with the Strang splitting method or an iterative splitting method, see [14] and [15].

One of the most popular and widely used operator-splittings is the so-called *Strang operator splitting (or Strang-Marchuk operator splitting)*, see [25], which takes the following form:

$$\begin{aligned} \frac{\partial c^*(t)}{\partial t} &= Ac^*(t), \text{ with } t^n \le t \le t^{n+1/2} \text{ and } c^*(t^n) = c^n_{\text{sp}}, \\ \frac{\partial c^{**}(t)}{\partial t} &= Bc^{**}(t), \text{ with } t^n \le t \le t^{n+1} \text{ and } c^{**}(t^n) = c^*(t^{n+1/2}), \\ \frac{\partial c^{***}(t)}{\partial t} &= Ac^{***}(t), \text{ with } t^{n+1/2} \le t \le t^{n+1} \text{ and } c^{***}(t^{n+1/2}) = c^{**}(t^{n+1}), \end{aligned} \tag{19}$$

where $t^{n+1/2} = t^n + \frac{1}{2}\tau_n$, and the approximation at the next time level t^{n+1} is defined as $c^{n+1}_{\text{sp}} = c^{***}(t^{n+1})$. The Strang formula can be constructed as

$$S_{Strang}(\Delta t, u^n) = \exp(\Delta t/2\ A)\exp(\Delta t\ B)\exp(\Delta t/2\ A)\ u_n. \tag{20}$$

The splitting error of the Strang splitting is

$$\text{err}_{\text{local}}(\tau_n) = \frac{1}{24}\tau_n^3([B,[B,A]] - 2[A,[A,B]])\ c^n_{\text{sp}} + \mathcal{O}(\tau_n^4), \tag{21}$$

$$\text{err}_{\text{global}}(\tau_n) = \frac{1}{24}\ t^{n+1}\ \tau_n^2([B,[B,A]] - 2[A,[A,B]])\ c^n_{\text{sp}} + \mathcal{O}(\tau_n^3), \tag{22}$$

see e.g. [25]. We see that this operator-splitting is also of second order. We note that under some special conditions for the operators A and B, the Strang splitting has third-order accuracy and can even be exact, see [25].

We can acchieve at least a fourth-order method by using the Richardson extrapolation.

We apply the Richardson extrapolation on the second-order Strang splitting method to obtain higher-order methods.

The idea of the extrapolation method is given as follows.

$$D_4(\Delta t, u^n) = u^{n+1,4th} = \frac{4}{3} S_{\text{Strang}}(\frac{\Delta t}{2}, S_{\text{Strang}}(\frac{\Delta t}{2}, u^n)) - \frac{1}{3} S_{\text{Strang}}(\Delta t, u^n) \quad (23)$$

where we have a fourth-order method ($O(\Delta t^4)$), see [24].

Remark 2. We can deal with first-, second-, and fourth-order splitting methods to obtain the proposed accuracy of the solutions. At least we have to balance the approximation error in time with the approxiamtion error in space. Often a first-order time splitting method is sufficient with a second-order dimensional splitting method, while the underlying spatial error is more dominant.

4.2 Dimensional Splitting Methods

Often it is important to split the dimensional directions. In our example the diffusion operator is predestinated for a dimensional splitting method.

We study the diffusion equation,

$$\begin{aligned} u_{tt} = D_1(x,y)u_{xx} + D_2(x,y)u_{yy} \ \text{ in } \Omega \times [0,T], \\ u(x,y,0) = u_0(x,y) \ \text{ on } \Omega, \\ u(x,y,t) = u_1(x,y,t) \ \text{ on } \partial\Omega \times [0,T]. \end{aligned} \quad (24)$$

The ADI method is given as

$$\begin{aligned} \left(L_x + \tfrac{\Delta t}{2} A_x\right) \Delta u^* = -\Delta t (L_y A_x + L_x A_y) u^n, \\ \left(L_y + \tfrac{\Delta t}{2} A_y\right) \Delta u = \Delta u^*, \end{aligned}$$

where $\Delta u^* = u^{n+1} - u^n$.

The following error estimates hold:

$$\begin{aligned} \left(L_x + \tfrac{\Delta t}{2} A_x\right) \left(L_y + \tfrac{\Delta t}{2} A_y\right) (u^{n+1} - u^n) = \\ = -\Delta t (L_x L_y A_x + L_x L_y A_y) u^n - \tfrac{\Delta t^3}{3} A_x A_y u^n, \end{aligned}$$

where the underlying fourth-order discretization in space is given as

$$\begin{aligned} L_x L_y u_{tt} = L_y A_x u_{xx} + L_x A_y u_{yy} + O(h^4) \ \text{ in } \Omega, \\ u(x,y,0) = u_0(x,y) \ , u_t(x,y,0) = u_1(x,y) \ \text{ in } \Omega, \\ u(x,y,t) = u_2(x,y) \ \text{ on } \partial\Omega, \end{aligned} \quad (25)$$

with

$$
\begin{aligned}
L_x &= 1 + \frac{h_x^2}{12}\delta_{xx}, \\
A_x &= D_1\delta_{xx}, \\
L_y &= 1 + \frac{h_y^2}{12}\delta_{yy}, \\
A_y &= D_2\delta_{yy},
\end{aligned}
$$

where $h = \max\{h_x, h_y\}$; δ_{xx} and δ_{yy} are the central difference operators for the second derivative.

Remark 3. The spatial decomposition method can be derived as a fourth-order method. So we have a more accurate scheme for the space methods as for the time methods. In our case, we have higher spatial errors then errors in time because of the coarse grid steps, and we need higher-order methods.

In the next section we discuss the numerical experiments.

5 Experiments for the Plasma Reactor

In the following we present the different models based on different scales. We distinguish between analytical and numerical models, so that we can directly solve simple models, or we propose numerical methods for more complex equations.

The next models can be solved analytically.

5.1 Stagnant Layer Model

In this model one assumes only the diffusion across a stagnant layer (mass-transfer-limited).

This model is used to simulate the gas transport of the concentration on a thin film. The contamination is given in the vertical direction. Based on the time-dependency, we can distinguish between a stationary and instationary model.

We model the transport of the contaminants by a convection-diffusion equation, that is given as

$$
\begin{aligned}
\frac{\partial c}{\partial t} = D(\frac{\partial^2 c}{\partial x^2} + \frac{\partial^2 c}{\partial y^2}) - v\frac{\partial c}{\partial x} \quad &\text{in } (x, y, t) \in [0, 1] \times [0, b] \times [0, \infty], \qquad (26) \\
c(x, y, 0) = 1 \quad &\text{on } (x, y) \in 0 \times [0, b], \\
c(x, y, t) = 0 \quad &\text{on } (x, y, t) \in [0, 1] \times 0 \times [0, \infty], \\
\frac{\partial c}{\partial y} = 0 \quad &\text{on } (x, y, t) \in [0, 1] \times b \times [0, \infty],
\end{aligned}
$$

where c is the concentration of the contaminant, D is the diffusion paramter of the idealized gas, v is the velocity in the x-direction of the gas. The dimension of the chamber is given as $\Omega = [0, 1] \times [0, b]$.

The following assumption is neccessary:
We assume a large flow rate or a large chamber, $vb >> D$.

The parameters are given for a first stationary experiment $t \to \infty$:

$$\begin{aligned} b &= 1.0, \\ v &= 0.1, \\ D &= 0.01. \end{aligned}$$

For the stationary solution, we obtain the following analytical solution:

$$c(x,y) = \frac{4}{\pi}\sin(\frac{\pi y}{2b})\exp(-\frac{\pi^2 Dx}{4vb^2}), \tag{27}$$

where $(x,y) \in [0,1] \times [0,1]$.

For the instationary solution, we obtain the following analytical solution:

$$c(x,y,t) = \frac{4}{\pi}\sin(\frac{\pi y}{2b})\exp(-\frac{\pi^2 D(x-vt)^2}{4vb^2}), \tag{28}$$

where $(x,y,t) \in [0,1] \times [0,b] \times [0,T]$, with $T \in \mathbb{R}^+$.

The growth rate is given as:

$$g = \frac{m_{\text{film}}}{m_{\text{gas}}}\frac{1}{\rho_{\text{film}}}j(x), \tag{29}$$

where $j(x)$ is the mass flux at substrate

$$j(x) = \frac{2}{b}D\exp(-\frac{\pi^2 Dx}{4vb^2}).$$

We simulate the analytical solution for the concentration and the growth.

Figure 1 presents the model in 2D.

Remark 4. The model can be used to have an overview to horizontal gas flows across the thin layer. We can compute the growth rate depending on the amount of the velocity and diffusion. The simulations are done with Maple and Mathematica.

5.2 Pulse Injection (Vertical Layer Model)

This model is used to simulate the transport with the x-axis. The pulse injection simulates a finite source. We can also rotate the model about 90 degrees to obtain the reactor configuration.

We have the following assumptions:
In this model, we assume that we have a pulse injection into a vertical gas chamber.

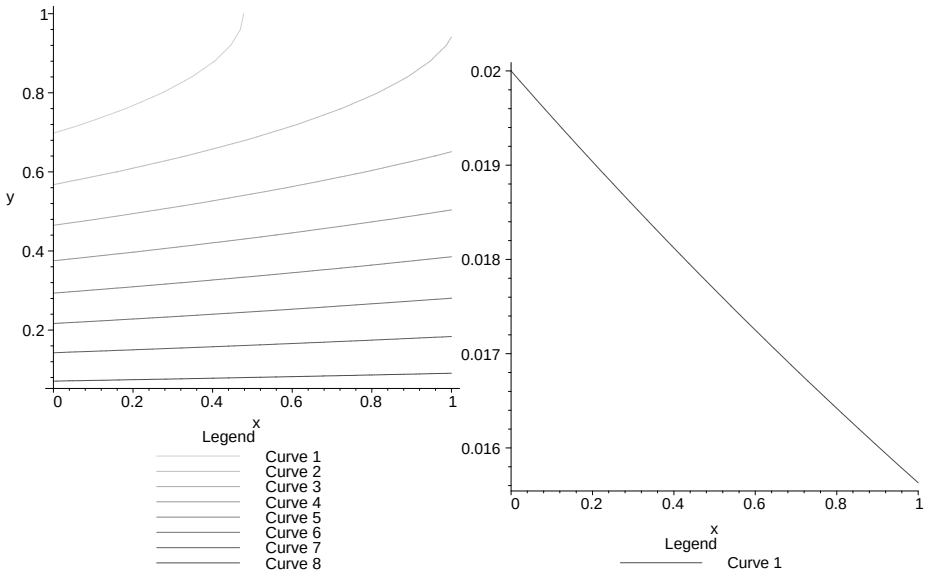

Fig. 1. 2D experiment of the stagnant layer. Left: gas concentration in the domain, right: growth rate of the thin film (paramters: $b = 1, v = 0.1, D = 0.01$, other parameters 1).

The convection-diffusion-reaction equation is given as:

$$\begin{aligned} \frac{\partial c}{\partial t} = (D_L \frac{\partial^2 c}{\partial x^2} + D_T \frac{\partial^2 c}{\partial y^2}) - v\frac{\partial c}{\partial y} - \lambda c, \ \text{ in } (x,y,t) \in [0,1] \times [0,b] \times [0,\infty] \quad (30) \\ c(x,y,0) = c_0 \ \text{ on } (x,y) = (x_0,y_0), \\ c(x,y,0) = 0 \ \text{ on } (x,y) \in \Omega \backslash \{(x_0,y_0)\}, \\ c(x,y,t) = 0 \ \text{ on } (x,y,t) \in \partial\Omega \times [0,\infty], \end{aligned}$$

where c is the concentration of the contaminant, the diffusion paramters are given as $D_L = \alpha_L v$, $D_T = \alpha_T v$, v is the velocity in x-direction. The decay rate is given as λ. The domain is given as $\Omega = [0,1] \times [0,1]$.

The parameters are given for the instationary experiment $t \to \infty$:

$$\begin{aligned} T &= 10.0, \\ v &= 0.1, \\ D &= 0.01, \\ c_0 &= 1.0. \end{aligned}$$

The analytical solution is given as

$$c(x,y,t) = \frac{c_0}{4\pi\sqrt{\alpha_L \alpha_T}(vt\pi)} \quad (31)$$

$$\exp(-\frac{((x-x_0)-vt)^2}{4\alpha_L vt})\exp(-\frac{(y-y_0)^2}{4\alpha_T vt})\exp(-\lambda t), \qquad (32)$$

where $(x, y) \in [0, 1] \times [0, 1]$, $t \in [0, T]$.

The growth rate is

$$g = \frac{m_{\text{film}}}{m_{\text{gas}}}\frac{1}{\rho_{\text{film}}}j(x), \qquad (33)$$

where $j(x)$ is the mass flux at substrate

$$j(y) = -D_L\frac{\partial c(x, y, t)}{\partial x})|_{x=0.1}.$$

We simulate the analytic solution for the concentration and the growth.

Figure 2 presents the model in 2D.

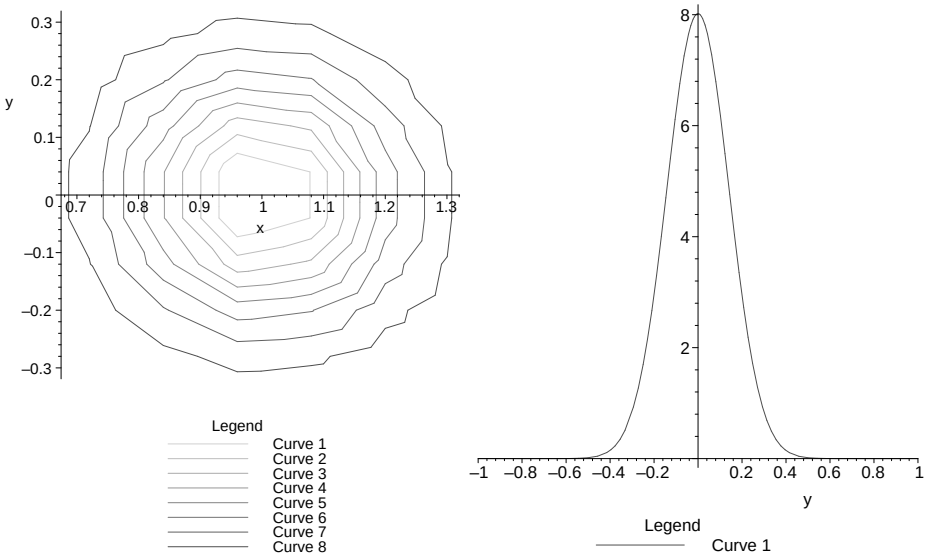

Fig. 2. 2D experiment of the vertical gas flow for the thin layer. Left: gas concentration in the domain, right: growth rate of the thin film (paramters : $v = 0.1, D = 0.01, \lambda = 0$, other parameters 1).

Remark 5. The model can be used to have an overview to vertical gas flows with a pulse injection across the thin layer. We can compute the growth rate depending on the amount of the velocity and diffusion. The simulations are done with Maple and Mathematica.

5.3 Point-Like Continuous Inflow (Vertical Layer Model)

This model is used to simulate the transport with the x-axis and to have an infinite source. We can also rotate the model about 90 degrees to obtain the reactor configuration.

We have the following assuptions:
In this model, we assume that we have a point-like continuous inflow into a vertical gas chamber.

The convection-diffusion equation is given as:

$$\begin{aligned}\frac{\partial c}{\partial t} = (D_L\frac{\partial^2 c}{\partial x^2} + D_T\frac{\partial^2 c}{\partial y^2}) - v\frac{\partial c}{\partial x} + q(t), \text{ in } (x,y,t) \in [0,1]\times[0,b]\times[0,\infty] \\ c(x,y,0) = 0 \text{ on } (x,y) \in 0\times[0,b], \\ c(x,y,t) = 0 \text{ on } (x,y,t) \in [0,1]\times 0\times[0,\infty], \\ \frac{\partial c}{\partial y} = 0 \text{ on } (x,y,t) \in [0,1]\times b\times[0,\infty],\end{aligned} \tag{34}$$

where $q(t) = \begin{cases} q_s/T, t \le T \\ 0, \quad t > T \end{cases}$ is the permanent inflow source at point $(x,y) = (0,0)$ and q_s is the source rate. T is the time for the injection. Further c is the concentration of the contaminant, the diffusion paramters are given as $D_L = \alpha_L v$, $D_T = \alpha_T v$, v is the velocity in x-direction. The decay rate is given as λ. The domain is given as $\Omega = [0,1]\times[0,1]$.

The parameters are given for a first experiment:

$$\begin{aligned}T &= 10.0, \\ v &= 0.1, \\ D &= 0.01, \\ q_s &= 1.0.\end{aligned}$$

The analytical solution is given as:

$$c(x,y,t) = \frac{q_s}{4\pi\sqrt{\alpha_l\alpha_T}}\exp(\frac{x}{2\alpha_L})W(\frac{r^2}{4\alpha_L v t}, \frac{r\gamma}{2\alpha_L}), \tag{35}$$

where $(x,y) \in [0,1]\times[0,1]$, $t \in [0,T]$, and with the Hantush function we have:

$$W(a_1,a_2) = \int_{a_1}^{\infty}\frac{1}{\zeta}\exp(-\zeta - \frac{a_2^2}{4\zeta}), \tag{36}$$

where

$$\begin{aligned}\gamma &= \sqrt{1 + 4\alpha_L\lambda/v}, \\ r &= \sqrt{x^2 + (\alpha_L/\alpha_T)y^2}.\end{aligned}$$

The growth rate is given as

$$g = \frac{m_{\text{film}}}{m_{\text{gas}}}\frac{1}{\rho_{\text{film}}}j(x), \tag{37}$$

where $j(x)$ is the mass flux at substrate

$$j(x) = -D\frac{\partial c(x,y,t)}{\partial x})|_{x=0.1}.$$

where $t = 100.0$. We simulate the analytic solution for the concentration and growth.

Figure 3 presents the model in 2D.

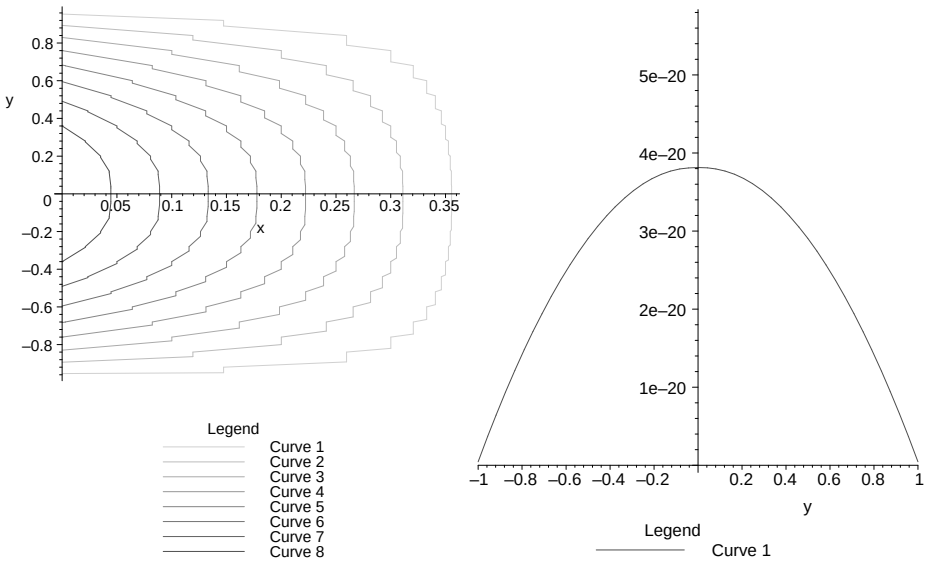

Fig. 3. 2D experiment of the vertical gas flow into the thin layer. Left: gas concentration in the domain, right: growth rate of the thin film (paramters : $v = 0.1, D = 0.01$, other parameters 1).

Remark 6. The model can be used to have an overview to vertical gas flows across the thin layer. We can compute the growth rate depending on the amount of the velocity and diffusion. The simulations are done with Maple and Mathematica.

The next models have more complicated initial and boundary conditions, also the geometry is more different, such that numerical methods are necessary to solve them.

5.4 Far Field Model: Large Mesoscopic Model

In this model one assumes small Knudson numbers. So we can describe our model with continuum equations. Since we want to model the flow very close to the wafer surface, we assume additionally that the flow is dominated by diffusion.

We have the following equation to simulate a first CVD process.

$$\begin{aligned} &\partial_t u + v \cdot \nabla u + \nabla \cdot D\nabla u = u_{\text{in}} \text{ in } \Omega \times (0,T), \\ &u_0(x,y) = 0 \text{ on } \Omega, \\ &\partial_t u(x,y,0) = u_1(x,y) = 0, \\ &u(x,y,t) = 0 \text{ on } \Gamma_1, \\ &v\frac{\partial u}{\partial n} = u_{\text{out}} \text{ on } \Gamma_2, \end{aligned} \tag{38}$$

where the constant inflow source is given as u_{in}. The bottom boundary Γ_2 is the outflow boundary, whereas the rest of the boundary Γ_1 is a Dirichlet boundary.

We discretize the spatial terms with finite volume methods and apply the BDF method for the time discretization.

Our time steps are given in the Courant number and we apply solver methods that are based on different grid levels, e.g. multi-grid methods.

Figure 4 presents the model in 2D.

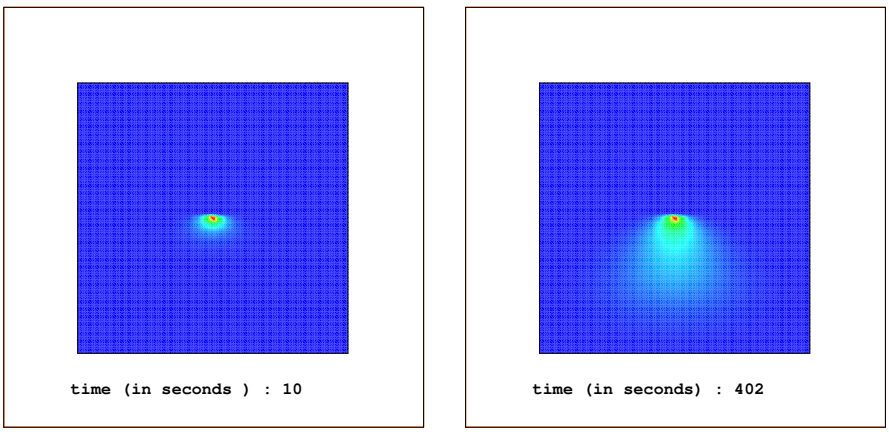

Fig. 4. 2D experiment of the apparatus with a single source.

The improved thin-film growth is given in Figure 5.

Remark 7. The model can be used to have an overview to vertical gas flows and the amount of sublimated concentration to the thin film. We can compute the growth rate depending on the outflow of the gas concentration. The simulations are done with Mathematica and numerically with UG.

Far Field Model: Fractal Sources for Improved Thin-Film Growth. We have the following equation to simulate the fractal sources. The equation is given

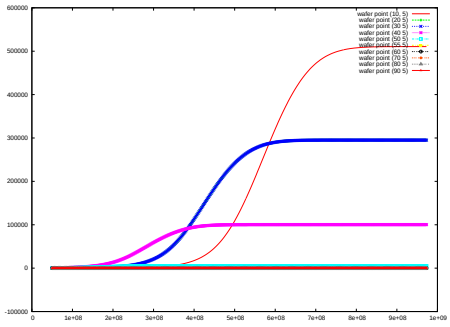

Fig. 5. Growth of the thin layer with single sources.

as

$$\partial_t u + v \cdot \nabla u + \nabla \cdot D \nabla u = \sum_{i=1}^{m} u_{\text{in}} \text{ in } \Omega \times (0,T), \tag{39}$$
$$u_0(x,y) = 0 \text{ on } \Omega,$$
$$\partial_t u(x,y,0) = u_1(x,y) = 0,$$
$$u(x,y,t) = 0 \text{ on } \Gamma_1,$$
$$v\frac{\partial u}{\partial n} = u_{\text{out}} \text{ on } \Gamma_2,$$

where the constant inflow sources are given as u_{in}^i, with $i = 1, \ldots, m$, whereas m is the number of sources. The bottom boundary Γ_2 is the outflow boundary, the rest of the boundary Γ_1 is a Dirichlet boundary.

We discretize the spatial terms with finite volume methods and apply the BDF method for the time discretization.

Our time steps are given in the Courant number and we apply solver methods that are based on different grid levels, e.g. multi-grid methods.

Figure 6 presents the model in 2D.

The improved thin-film growth is given in Figure 7.

Remark 8. The model can be used to optimize the ordering of the fractal sources. To obtain a nearly equivalent thin film, the sources have to be arranged in different layers, with decreasing amount of inflow.

5.5 Three-Dimensional Far Field Model: Large Mesoscopic Model

The discussion about the growth of the thin layer in three dimensions is important. In this model, we assume small Knudson numbers. So we can describe our model with continuum equations. Since we want to model the flow very close to the wafer surface, we assume additionally that the flow is dominated by diffusion.

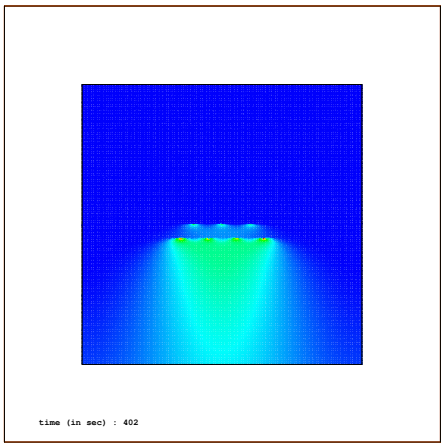

Fig. 6. 2D experiment of the apparatus with fractal sources.

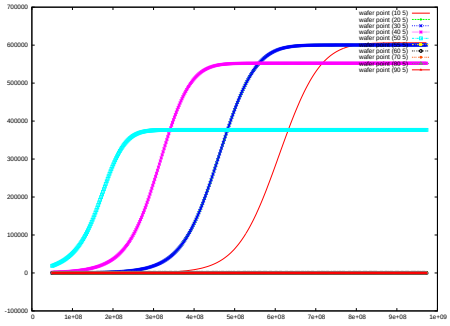

Fig. 7. Growth of the thin layer with fractal sources.

We have the following equation to simulate a first CVD process. The equation is given as

$$\begin{aligned}
&\partial_t u + v \cdot \nabla u + \nabla \cdot D\nabla u = u_{\text{in}} \text{ in } \Omega \times (0,T), \\
&u_0(x,y) = 0 \text{ on } \Omega, \\
&\partial_t u(x,y,0) = u_1(x,y) = 0, \\
&u(x,y,t) = 0 \text{ on } \Gamma_1, \\
&v\frac{\partial u}{\partial n} = u_{\text{out}} \text{ on } \Gamma_2,
\end{aligned} \tag{40}$$

where the constant inflow source is given as u_{in}. The bottom boundary Γ_2 is the outflow boundary, whereas the rest of the boundary Γ_1 is of Dirichlet type.

We discretize the spatial terms with finite volume methods and apply the BDF method for the time discretization. Further we apply characteristics methods for the convection term.

Our time steps are given in the Courant number and we apply solver methods that are based on different grid levels, e.g. multi-grid methods.

Figure 8 presents the model in 3D.

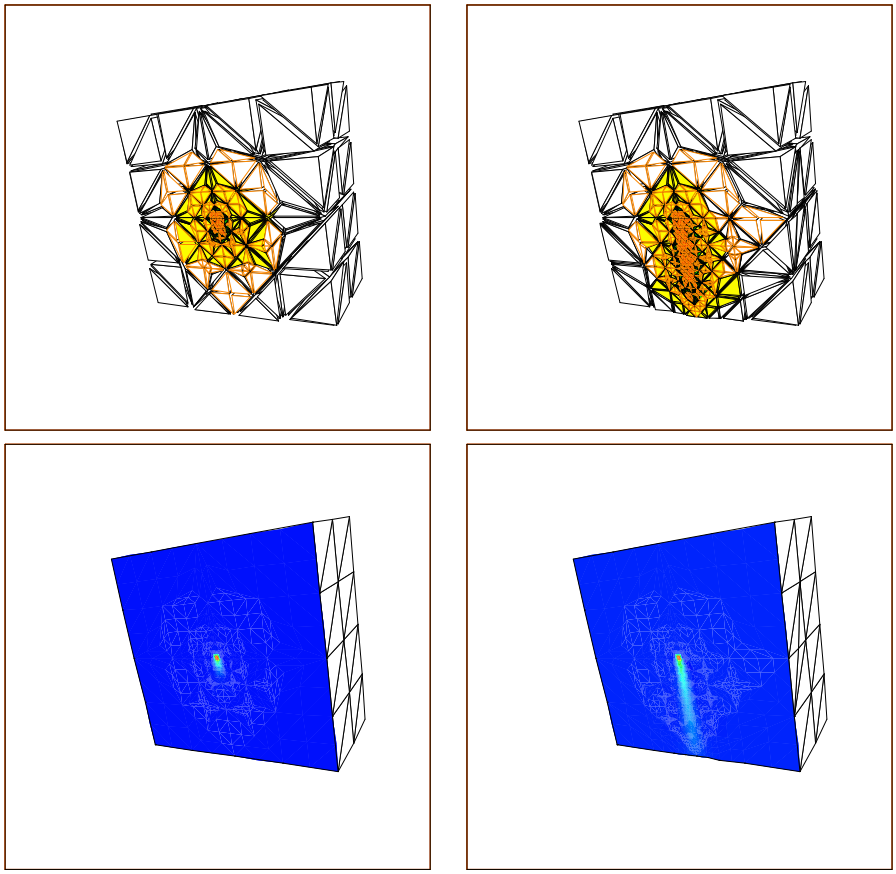

Fig. 8. 3D experiment of the apparatus with a single source.

The improved thin-film growth is given in Figure 9.

Remark 9. The model can be used to have an overview to vertical gas flow in three dimensions. We can compute the growth rate depending on the outflow of the gas concentration. The adaptivity allows to compute fine regions of the flow.

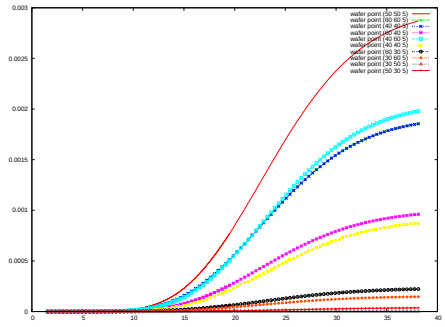

Fig. 9. Growth of the thin layer with single sources in 3d.

The simulations were done with 150,000 elements using the software package UG.

6 Conclusions and Discussions

We present a continuous or kinetic model, due to the far field or near field effect. Based on the different scale models we could predict the flow of the reacting chemicals on the scale of the chemical reactor. For the mesoscopic scale model we discussed the discretization and solver methods. Numercial examples are presented to discuss the influence of the near-continuum regime at the thin film. The modeling of various inflow sources can discribe the growth of the thin film at the wafer. In future, we will analyze the validity of the models with physical experiments.

References

1. J.C. Butcher. *Numerical Methods for Ordinary Differential Equations.* John Wiley & Sons Ltd, Chichester, (2003).
2. P. Csomós, I. Faragó and A. Havasi. *Weighted sequential splittings and their analysis.* Comput. Math. Appl., (to appear)
3. K.-J. Engel, R. Nagel, *One-Parameter Semigroups for Linear Evolution Equations.* Springer, New York, 2000.
4. I. Farago. *Splitting methods for abstract Cauchy problems.* Lect. Notes Comp.Sci. 3401, Springer Verlag, Berlin, 2005, pp. 35-45
5. I. Farago, J. Geiser. *Iterative Operator-Splitting methods for Linear Problems.* Preprint No. 1043 of the Weierstrass Institute for Applied Analysis and Stochastics, Berlin, Germany, June 2005.
6. I. Farago, A. Havasi. *On the convergence and local splitting error of different splitting schemes.* Eötvös Lorand University, Budapest, 2004.
7. P. Frolkovič and H. De Schepper. *Numerical modelling of convection dominated transport coupled with density driven flow in porous media.* Advances in Water Resources, 24:63–72, 2001.

8. P. Frolkovič. *Flux-based method of characteristics for contaminant transport in flowing groundwater.* Computing and Visualization in Science, 5(2):73-83, 2002.
9. E. Hairer, S.P. Norsett, and G. Wanner. *Solving Ordinary Differential Equatons I.* SCM, Springer-Verlag Berlin-Heidelberg-New York, No. 8, 1992.
10. W. Hundsdorfer and J.G. Verwer. *Numerical solution of time-dependent advection-diffusion-reaction equations*, Springer, Berlin, (2003).
11. J. Geiser. *Numerical Simulation of a Model for Transport and Reaction of Radionuclides.* Proceedings of the Large Scale Scientific Computations of Engineering and Environmental Problems, Sozopol, Bulgaria, 2001.
12. J. Geiser. *Gekoppelte Diskretisierungsverfahren für Systeme von Konvektions-Dispersions-Diffusions-Reaktionsgleichungen.* Doktor-Arbeit, Universität Heidelberg, 2003.
13. J. Geiser. *Discretization methods with analytical solutions for convection-diffusion-dispersion-reaction-equations and applications.* Journal of Engineering Mathematics, published online, Oktober 2006.
14. J. Geiser. *Linear and Quasi-Linear Iterative Splitting Methods: Theory and Applications.* International Mathematical Forum, Hikari Ltd., 2, no. 49, 2391 - 2416, 2007.
15. J. Geiser. *Decomposition Methods for Partial Differential Equations: Theory and Applications in Multiphysics Problems.* Habilitation Thesis, Humboldt University of Berlin, Germany, under review, June 2007.
16. M.K. Gobbert and C.A. Ringhofer. *An asymptotic analysis for a model of chemical vapor deposition on a microstructured surface.* SIAM Journal on Applied Mathematics, 58, 737–752, 1998.
17. H.H. Lee. *Fundamentals of Microelectronics Processing* McGraw-Hill, New York, 1990.
18. M.A. Lieberman and A.J. Lichtenberg. *Principle of Plasma Discharges and Materials Processing.* Wiley-Interscience, AA John Wiley & Sons, Inc Publication, Second edition, 2005.
19. Chr. Lubich. *A variational splitting integrator for quantum molecular dynamics.* Report, 2003.
20. S. Middleman and A.K. Hochberg. *Process Engineering Analysis in Semiconductor Device Fabrication* McGraw-Hill, New York, 1993.
21. M. Ohring. *Materials Science of Thin Films.* Academic Press, San Diego, New York, Boston, London, Second edition, 2002.
22. A.E. Scheidegger. *General theory of dispersion in porous media.* Journal of Geophysical Research, 66:32–73, 1961.
23. T.K. Senega and R.P. Brinkmann. *A multi-component transport model for non-equilibrium low-temperature low-pressure plasmas.* J. Phys. D: Appl.Phys., 39, 1606–1618, 2006.
24. J. Stoer and R. Burlisch. *Introduction to Numerical Analysis.* 3rd. ed. , Springer-Verlag, New-York, 2002.
25. G. Strang. *On the construction and comparision of difference schemes.* SIAM J. Numer. Anal., 5:506–517, 1968.